Non-invasive Assessment of Coronary Artery Disease in Arterial Bifurcations: A Comparative Study of CCTA, CFD, and Fractional Flow Reserve Measurements

Andreas G. Stavroulis, Georgios N. Papadopoulos, Ioannis T. Anastasopoulos, Dimitrios K. Vasilopoulos, Nikolaos P. Theodorakis

Department of Biomedical Engineering, Aristotle University of Thessaloniki, GR54124 Thessaloniki, Greece; Department of Cardiology, University Hospital of Patras, GR26504 Patras, Greece; Computational Mechanics Laboratory, National Technical University of Athens, GR15780 Athens, Greece

Abstract. Recent advances in coronary computed tomography angiography (CCTA) allow the calculation of various functional indices of coronary artery disease (CAD). smartFFR is our proposed new index for the assessment of the significance of coronary stenoses in coronary bifurcations. The aim of the current study is to compare smartFFR with the Fractional Flow Reserve (FFR) values deriving from direct invasive pressure measurements from a dedicated pressure wire. In the context of the SMARTool study, 22 patients with chest pain symptoms and intermediate pre-test likelihood of CAD underwent CCTA as well as FFR measurement. The 22 left arterial branches which included the LAD and the LCx were reconstructed using our in-house developed software. We performed two computational blood flow simulations for each case to calculate the smartFFR for each 3D model. Regarding the inlet, the average patient-specific pressure at rest was applied as a boundary condition. Assuming a myocardial blood flow of 2 ml/s and 6 ml/s during rest and under stress for the Left Main artery, respectively, we calculated the flow for each branch using Murray's law and applied it as outlet boundary conditions. smartFFR was calculated for each branch by computing the ratio of distal to proximal pressure for a range of flows between 0 and 4 ml/s, normalized by the respective ratio of a normal artery. The required average process time was less than 20 minutes. Strong correlation ($r=0.88$, $P<0.0001$) was found between the two methods. All pathological cases presenting ischemia, were correctly categorized by our method as hemodynamically significant lesions. smartFFR demonstrated a high diagnostic accuracy for distinguishing hemodynamically significant lesions in a matter of minutes, and may represent a valid non-invasive tool for comprehensive characterization of CAD. **Keywords:** smartFFR, FFR, CCTA.

1 Introduction

The modern lifestyle in westernized societies has constituted cardiovascular diseases as one of the most common causes of death. Thus, the development of non-invasive techniques for the hemodynamic assessment of coronary arteries is of tremendous importance in modern clinical practice.

So far, the technique which is considered as the gold standard in the functional assessment of coronary arteries is the fractional flow reserve measurement (FFR). FFR is an invasive technique which requires the use of a dedicated pressure-flow wire, as well as the induction of hyperemia after the intravenous administration of adenosine. FFR is the ratio of the intravascular pressure distal of the stenosis divided by the respective aortic pressure. An FFR value 0.80 is considered as the threshold below which, the diseased artery is in need of a percutaneous coronary intervention (PCI).

Regarding coronary imaging modalities, the most commonly used in everyday clinical practice is the traditional invasive coronary angiography (ICA). ICA is a semiinvasive imaging technique which allows the 2-dimensional representation of the coronary vasculature after the insertion of the proper contrast media. Another coronary imaging modality that has gained substantial ground during the past decade due to its non-invasive nature is the coronary computed tomography angiography (CCTA). CCTA manages to give a visual representation of the coronary vasculature and provide useful information on the severity of a coronary stenosis, as well as, the type and extent of any possible atherosclerotic plaques.

The ongoing development of 3D reconstruction methods, combined with the application of computational fluid dynamics (CFD) on the 3D models has allowed the calculation of important hemodynamic parameters such as intravascular pressures, therefore allowing also the hemodynamic assessment of the artery of interest. Numerous studies have been published regarding the computational assessment of coronary stenosis [1-5]. The aforementioned methods suffer mainly of two drawbacks, the long computational time that is required to execute the flow simulations and the need of a remote core-laboratory analysis. Another drawback of other methods is the inability to be applied on bifurcating arterial models, since they can only generate results segmentally.

In the current study, we propose a new method for the computational functional assessment of coronary stenosis on 3D models of bifurcating arteries, and more specifically on models that include the left coronary artery (i.e. Left Anterior Descending and Left Circumflex). 18 patients were used to reconstruct in 3D their respective left coronary vasculature using our in-house developed algorithm and the smartFFR index was calculated in all 18 branches. The smartFFR values of the 22 arteries was compared against the invasively measured FFR.

2 Materials and Methods

Dataset

In the context of the SMARTool project, a group of 18 symptomatic patients with intermediate pre-test probability (20–90%) of CAD underwent a CCTA exam (64-slice General Electric Medical Systems Discovery PET/CT 690® scanner) and a FFR measurement (ComboWire, Volcano Corp, Rancho Cordova, CA). All 18 left coronary branches were reconstructed. However, the smartFFR was calculated only for the branches that had an invasively measured FFR value (i.e. 22 cases).

3D Reconstruction Process

The 3D reconstruction of the 18 arterial branches was performed using our in-house developed reconstruction algorithm [6].

In brief, the reconstruction algorithm is based on a six-stage approach: a) The CCTA images are pre-processed

b) The arterial borders are initially detected

c) The arterial centerline is extracted using a minimum cost path approach

d) The lumen parameters are translated and adapted into Hounsfield units (HU)

e) An enhancement of the active contours model is implemented for the lumen segmentation

f) The 3D surface for the lumen is created (Figure 1)

The coronary branches were reconstructed using the same landmarks for all patients. The segmentation of the branches was based on the SYNTAX SCORE chart. More specifically, regarding the LAD we included segments 1-3, whereas for the LCx we included segments 11-13.

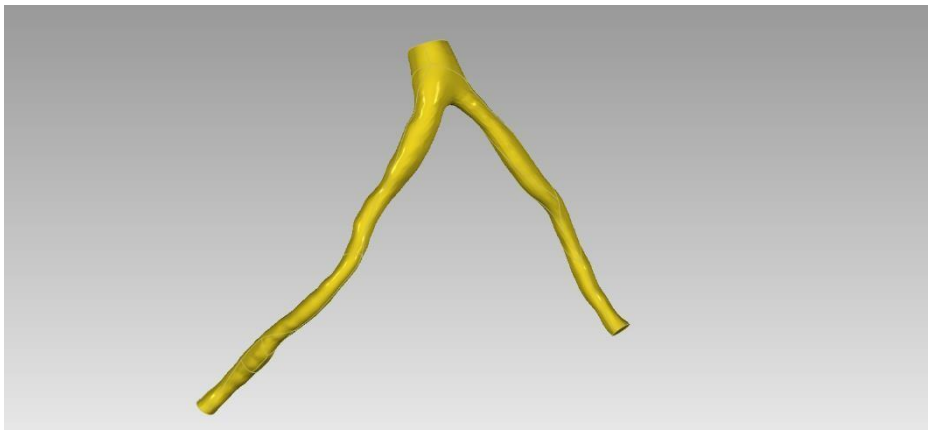

Figure 1: Final 3D reconstructed model of a left arterial branch.

smartFFR calculation process

To validate the proposed method, we performed the smartFFR calculations on 18 arterial branches, having 22 vessels in total (i.e. also with an invasive FFR measured). Our simulations were performed under the assumption that the arterial wall was rigid, thus not taking into account its interaction with the blood flow. Blood flow was modelled using the Navier-Stokes and the continuity equations:

$$\rho \frac{\partial \mathbf{v}}{\partial t} + \rho(\mathbf{v}\cdot\nabla)\mathbf{v} = \nabla\cdot\boldsymbol{\tau} + \mathbf{f}, \quad (1)$$

$$\nabla\cdot(\rho\mathbf{v}) = 0, \quad (2)$$

where $\mathbf{v}$ is the blood velocity vector and $\boldsymbol{\tau}$ is the stress tensor, which is defined as:

$$\boldsymbol{\tau} = -p\mathbf{I} + 2\mu\varepsilon_{ij}, \quad (3)$$

where δ_{ij} is the Kronecker delta, μ is the blood dynamic viscosity, p is the blood pressure and ε_{ij} is the strain tensor calculated as:

$$\varepsilon_{ij} = \frac{1}{2}\left(\nabla\mathbf{v} + (\nabla\mathbf{v})^T\right), \quad (4)$$

Blood was modelled as a Newtonian fluid with density 1050 kg/m^3 and dynamic viscosity 0.0035 Pa·s. Blood flow was considered laminar and the Reynolds number ranged from 245–1832.

Boundary Conditions

For each case, we performed two blood flow simulations. In the inlet, we applied an average pressure of 100 mmHg which is considered as the average aortic pressure of a human under rest. At the wall a no-slip, no penetration boundary condition was imposed, thus assuming that the velocity of blood at the interface between the blood and the arterial wall is zero.

Regarding the outlet, we used two different flow rates as an outflow boundary condition. According to several flow measurements deriving from PET perfusion, the average flow during rest at the left coronary artery (i.e. starting from the Left Main branch and bifurcating to the respective LAD and LCx arteries) is 2 ml/s, whereas under stress, the respective value reaches an average of 6 ml/s. in order for us to determine the ratio under which flow is divided at the bifurcation site, we applied Murray's law for each case.

In general, Murray's law correlates the flow ratio through the side branches with the diameters of the branches. This relation is given by:

$$q_{D2} : d_{D2}^{3} , \quad (5)\ q_{D1} \cdot d_{D1}^{3} \cdot$$

with q_{D1} and q_{D2} the flow through and d_{D1} and d_{D2} the diameters of the branches which are calculated directly from the 3D models.

The calculated flow rates were then imposed as outflow boundary conditions for each of the two simulations. Then, for each simulation the pressure gradient of each branch was calculated in order to build the patient-specific P_d/P_a vs. flow curve [6]:

$$\frac{P_d}{P_a} = 1 - f_v \frac{Q}{P_a} - f_s \frac{Q^2}{P_a} \quad (6)$$

where Q is the flow rate, f_v is the coefficient of pressure loss due to viscous friction and f_s is the coefficient of pressure loss due to flow separation. Using P_a=100 mmHg in Eq. (6) allows the calculation of the two previously unknown coefficients, thus leading to the calculation of the area under the patient-specific P_d/P_a vs. flow curve. Finally, smartFFR is then calculated as the ratio of the area under the patient-specific P_d/P_a vs. flow curve to the respective reference area (i.e. the respective curve of a healthy artery).

Mesh

All 3D models were discretized using the same mesh parameters. In general, the arterial models were discretized into tetrahedral elements with a face size between 0.09 and 0.1 mm, resulting to models of around 5 million elements. This specific element size was chosen after a mesh sensitivity analysis.

3 Results

We examined the validity of our newly proposed method by comparing the smartFFR values against the respective invasively measured FFR values. Strong correlation was found between the two methods (Pearson correlation coefficient r=0.88, P<0.001) (Figure 3). Moreover, good agreement was also observed, using the Bland–Altman method of comparison (Difference = −0.02864±0.059, p=0.034) (Figure 2). A small overestimation of smartFFR was also observed (Mean difference=−0.02864). Finally, we also performed a Receiver Operator Curve (ROC) analysis to identify the optimal threshold for smartFFR to identify ischemic lesions that require a PCI (Figure 4). The smartFFR threshold was ≤0.83 (i.e. deriving from the Youden index) to identify cases with FFR≤0.8 (AUC=0.986, P<0.001). The accuracy, sensitivity, specificity, Positive Predictive Value (PPV) and Negative Predictive Value (NPV) were 90.9%, 100%, 86.7%, 77.8% and 100%, respectively (Table 1).

Table 1: Per-vessel diagnostic performance for smartFFR ≤ 0.83

Accuracy	Sensitivity	Specificity	PPV	NPV
90.9%	100%	86.7%	77.8%	100%

4 Discussion

In this work we presented our newly proposed computational functional assessment index which can be applied on 3D models of coronary branches. 18 patients were selected for this study that underwent a CCTA exam and FFR measurement in at least one of the two main left arterial branches. 22 smartFFR values were compared to the invasively measured FFR values in order to validate the proposed method. The results were very promising, presenting strong correlation and good agreement between the two methods. smartFFR presented a slight overestimation of the FFR. This can be attributed to the fact that our method strictly relies on geometrical factors and does not take into account the microcirculatory system. The unique advantage of the proposed method is the very low computational time that is needed for each case, since less than an average of 20 minutes is required for the whole procedure. Moreover, the induction of hyperemia is redundant since the whole procedure is fully computational. Another point that needs to be noted is the fact that the whole process does not require a remote core-laboratory analysis and can be performed on any computer with average computational power.

One limitation of the present study is the rather modest dataset that was used which however, was counterbalanced by the quality of the dataset, since 7 of the 22 cases were pathological (i.e. 32%). A second limitation of the whole procedure is that in heavily calcified cases, the arterial lumen is underestimated because of the so-called blooming effect, thus affecting the final calculated smartFFR value.

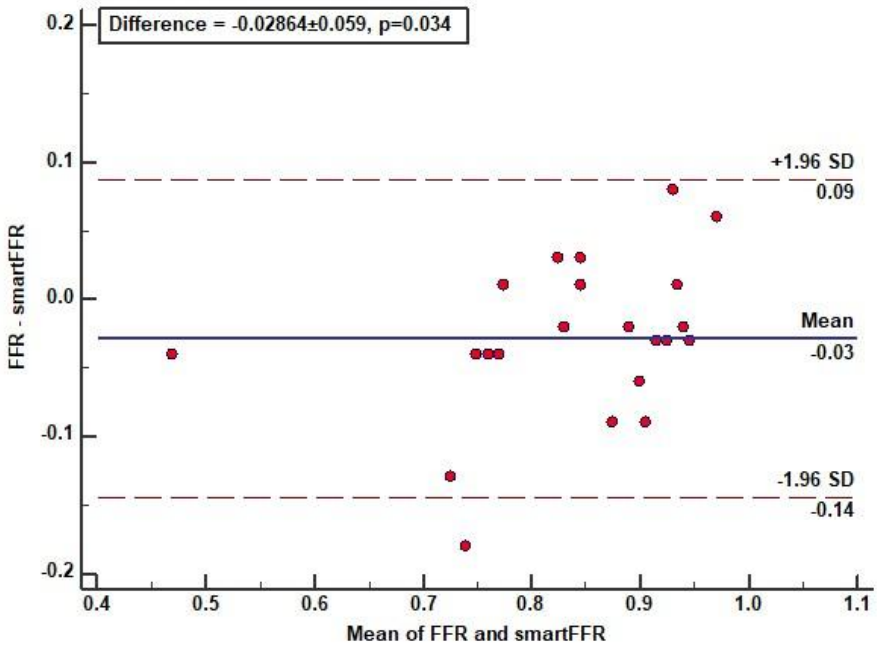

Figure 2: Bland-Altman plot comparing smartFFR to the invasively measured FFR.

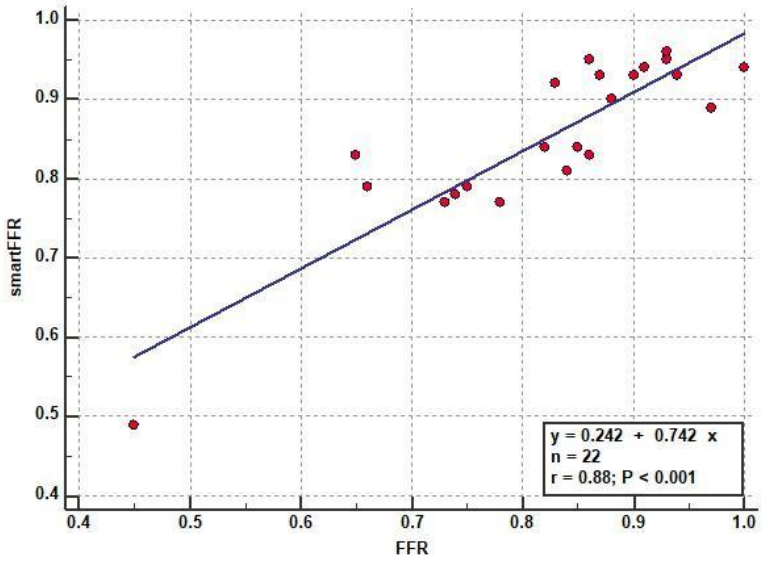

Figure 3: Regression plot for smartFFR and the invasively measured FFR.

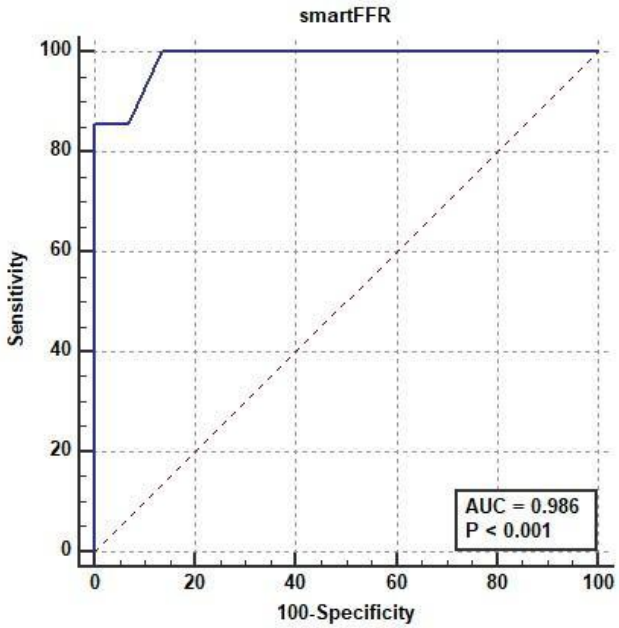

Figure 4: ROC curve for the smartFFR method.

5 Conclusions

The results of the current study suggest that the smartFFR can be accurately applied in coronary branches and can correctly discriminate a stenosis as hemodynamically significant or non-significant.

References

1. M. Renker, U. J. Schoepf, R. Wang, F. G. Meinel, J. D. Rier, R. R. Bayer, et al., "Comparison of Diagnostic Value of a Novel Noninvasive Coronary Computed Tomography Angiography Method Versus Standard Coronary Angiography for Assessing Fractional Flow Reserve," American Journal of Cardiology, vol. 114, pp. 1303-1308, Nov 1 2014.
2. M. Kruk, L. Wardziak, M. Demkow, W. Pleban, J. Pregowski, Z. Dzielinska, et al., "Workstation-Based Calculation of CTA-Based FFR for Intermediate Stenosis," JaccCardiovascular Imaging, vol. 9, pp. 690-699, Jun 2016.
3. J. K. Min, J. Leipsic, M. J. Pencina, D. S. Berman, B. K. Koo, C. van Mieghem, et al., "Diagnostic Accuracy of Fractional Flow Reserve From Anatomic CT Angiography," Jama-Journal of the American Medical Association, vol. 308, pp. 1237-1245, Sep 26 2012.
4. P. D. Morris, D. Ryan, A. C. Morton, R. Lycett, P. V. Lawford, D. R. Hose, et al., "Virtual fractional flow reserve from coronary angiography: modeling the significance of coronary lesions: results from the VIRTU-1 (VIRTUal Fractional Flow Reserve From Coronary Angiography) study," JACC Cardiovasc Interv, vol. 6, pp. 149-57, Feb 2013.
5. M. I. Papafaklis, T. Muramatsu, Y. Ishibashi, L. S. Lakkas, S. Nakatani, C. V. Bourantas, et al., "Fast virtual functional assessment of intermediate coronary lesions using routine angiographic data and blood flow simulation in humans: comparison with pressure wire - fractional flow reserve," EuroIntervention, vol. 10, pp. 574-83, Sep 2014.
6. L. Athanasiou, G. Rigas, A. I. Sakellarios, T. P. Exarchos, P. K. Siogkas, C. V. Bourantas, et al., "Three-dimensional reconstruction of coronary arteries and plaque morphology using CT angiography--comparison and registration with IVUS," BMC Med Imaging, vol. 16, p. 9, 2016.